Cu(I)-Glutathione Assembly Supported on ZIF-8 as Robust and Efficient Catalyst for Mild CO2 Conversions

Wenjuan Wang, Tiansheng Wang, Shuang Chen, Ying Lv, L. Salmon, Bruno Espuche, Sergio Moya, Oksana Morozova, Yapei Yun, Desirè Di Silvio, et al.

How to cite: *Angew. Chem. Int. Ed.* **2024**, *63*, e202407430
doi.org/10.1002/anie.202407430

Heterogeneous Catalysis

Cu(I)-Glutathione Assembly Supported on ZIF-8 as Robust and Efficient Catalyst for Mild CO_2 Conversions

Wenjuan Wang[+], Tiansheng Wang[+], Shuang Chen, Ying Lv, Lionel Salmon, Bruno Espuche, Sergio Moya, Oksana Morozova, Yapei Yun, Desiré Di Silvio, Nathalie Daro, Murielle Berlande, Philippe Hapiot, Jean-Luc Pozzo, Haizhu Yu, Jean-René Hamon,* and Didier Astruc**

Abstract: The Cu-glutathione (GSH) redox system, essential in biology, is designed here as a supramacromolecular assembly in which the tetrahedral 18e Cu(I) center loses a thiol ligand upon adsorption onto ZIF-8, as shown by EXAFS and DFT calculation, to generate a very robust 16e planar trigonal single-atom Cu(I) catalyst. Synergy between Cu(I) and ZIF-8, revealed by catalytic experiments and DFT calculation, affords CO_2 conversion into high-value-added chemicals with a wide scope of substrates by reaction with terminal alkynes or propargyl amines in excellent yields under mild conditions and reuse at least 10 times without significant decrease in catalytic efficiency.

The Cu-glutathione(GSH) redox system plays a key role in cellular homeostasis, detoxification and signaling due to the GSH affinity for Cu(I), present in the intra-cellular environment, GSH being the most abundant thiol in cells.[1]

In this context, we report here the new suprametallomacromolecular ensemble Cu(I)-GSH supported on ZIF-8 as a remarkably robust catalyst for the very efficient carboxylation reactions of terminal alkynes and cyclization of propargyl amines under atmospheric CO_2 pressure and mild conditions. This includes strong positive synergetic effect between Cu(I)-GSH and ZIF-8. Indeed, in order to fulfill the circular carbon economy, immense effort has been dedicated to CO_2 capture and utilization.[2] Up to now, various in-depth investigations have been implemented on producing, from CO_2, products such as terminal alkyne acids, polycarbonates, cyclic carbonates, etc.[3] The carboxylation of terminal alkynes with CO_2 and the cyclization of propargyl amines with CO_2 appear to be a good global market value, because of wide applications of propionic acid derivatives and oxazolidinones in cosmetics, pharmaceuticals, and plastics.[4] Therefore, known catalysts include inter alia nanoparticles (NPs) in metal–organic frameworks (MOFs) and covalent organic frameworks (COFs).[5] Most catalysts are noble-metal-based, but, for wide applications, the use of such costly and rare noble metals should, as much as possible, be avoided. Recently, Zhao's group reported the catalyst Cu_2O@ZIF-8 for conversion of propargylic alcohols and propargylic amines with CO_2.[6] However, copper oxides have long been known to increase the level of toxic reactive oxygen species (ROS) in human tissues[7] and contribute to cell death by inflicting toxic effects on two of the most important cell organelles including the mitochondria and lysosome. Concentration of copper oxide NPs facing human exposure levels can suppress the human immune system by

[*] Dr. W. Wang,[+] T. Wang,[+] M. Berlande, Prof. Dr. J.-L. Pozzo, Prof. Dr. D. Astruc
University of Bordeaux, ISM, UMR CNRS N°5255
351 Cours de La Libération, 33405 Talence Cedex, France
E-mail: didier.astruc@u-bordeaux.fr

Dr. W. Wang,[+] Dr. P. Hapiot, Dr. J.-R. Hamon
Univ. Rennes, CNRS, ISCR (Institut des Sciences Chimiques de Rennes) UMR 6226, 35000 Rennes, France
E-mail: jean-rene.hamon@univ-rennes1.fr

T. Wang,[+] Dr. L. Salmon
LCC, CNRS UPR 8241 & University of Toulouse, 31077 Toulouse Cedex, France

Prof. Dr. S. Chen, Y. Lv, Dr. Y. Yun, Prof. Dr. H. Yu
Department of Chemistry and Center for Atomic Engineering of Advanced Materials, Anhui Province Key Laboratory of Chemistry for Inorganic/Organic Hybrid Functionalized Materials, Anhui University, Hefei, Anhui, 230601 People's Republic of China
E-mail: yuhaizhu@ahu.edu.cn

Dr. B. Espuche, Dr. S. Moya, O. Morozova
Soft Matter Nanotechnology Lab, CIC biomaGUNE, Paseo Miramón 182, 20014 Donostia-San Sebastián, Gipuzkoa, Spain

Dr. B. Espuche
POLYMAT, Applied Chemistry Department, Faculty of Chemistry, University of the Basque Country, UPV/EHU, Paseo Manuel de Lardizabal 3, Donostia-San Sebastián, 20018, Spain

Dr. D. Di Silvio
CIC biomaGUNE, Paseo Miramón 194, 20014 Donostia/San Sebastián, Gipuzkoa, Spain

Dr. N. Daro
University of Bordeaux, CNRS, Bordeaux INP, ICMCB, UMR 5026, 33600 Pessac, France

[+] Both authors (WW and TW) contributed equally to this work.

cell death induction in lymphocytes.[7,8] In order to overcome these obstacles, we have envisaged the design of "green" oxide-free Cu(I)-GSH supported on zeolitic imidazolate framework (ZIF)-8, GSH being known as an inhibitor of Cu-induced toxicity in living organisms.[7a]

Although, under biological conditions, an adamantane-like $Cu(I)_4(GS)_6$ structure was proposed with deprotonated GS sulfhydryl groups as ligands, the Cu(I)-GSH structure depends on reaction conditions.[1c] Thus, Cu(I)-GSH/ZIF-8 (Figure 1) was synthesized by first reducing $Cu(NO_3)_2$ with Na ascorbate to produce 1.9 ± 0.5 nm nanoparticles (Figure S1a), etching with GSH to form Cu(I)-GSH,[9] then wet-impregnation onto ZIF-8[10] at 20 °C (Figure 1a). Extended X-ray absorption fine structure (EXAFS, Figure 1c–e and X-ray photoelectron spectroscopy (XPS, Figure 1f) of both Cu(I)-GSH and Cu(I)-GSH/ZIF-8, transmission electron microscopy (TEM) and electrochemistry (Figure 1c–g, S1b-d and S9) show the absence of cluster or metal-metal bonded structure and the presence of Cu(I). EXAFS (Table S1) reveals the presence of two strong Cu–O or Cu–N bonds in both nanomaterials, and a number of C–S bonds decreasing from two for Cu(I)-GSH to only one in Cu(I)-GSH/ZIF-8. This latter variation upon adsorption onto ZIF-8 suggests weakness of these Cu–S bonds. The Cu–S bond is shown by the restricted rotation around the S-linked cysteine (Cys) CH–CH_2 bond, each of the two diastereotopic CH_2 protons $H_{d'}$ and $H_{d''}$, in Cu(I)-GSH, appearing as four lines at 2.9 resp. 3.1 ppm in ^{1}H NMR (D_2O) resulting from mutual coupling ($^2J=14.3$ Hz) and distinct coupling with the viscinal CH proton ($^3J_{CH-CHd'}=4.6$ Hz; $^3J_{CH-CHd''}=9.4$ Hz, Figure S4). The time-of-flight mass spectrum shows a single major peak for Cu_2L_2 (L = Cys thiol), consistent with Cu(I) coordination at two GSH sites assigned to thiol and aminocarboxyl insuring the metalllopolymer structure (Figure 1a, S1 and S7). The latter is confirmed by irradiation of the UV/Vis. absorption band at 280 nm resulting in the appearance of a broad emission signal around 400 nm characterizing an assembly[11] represented in Figure 1a and S8. From the two CO_2H groups of glutamic acid (Glu) and glycine (Gly) of GSH, the deprotonated one (infrared: 1638 cm^{-1}) is coordinated to Cu, the Glu one being much favored, because it forms the robust 5-membered chelating aminocarboxylate

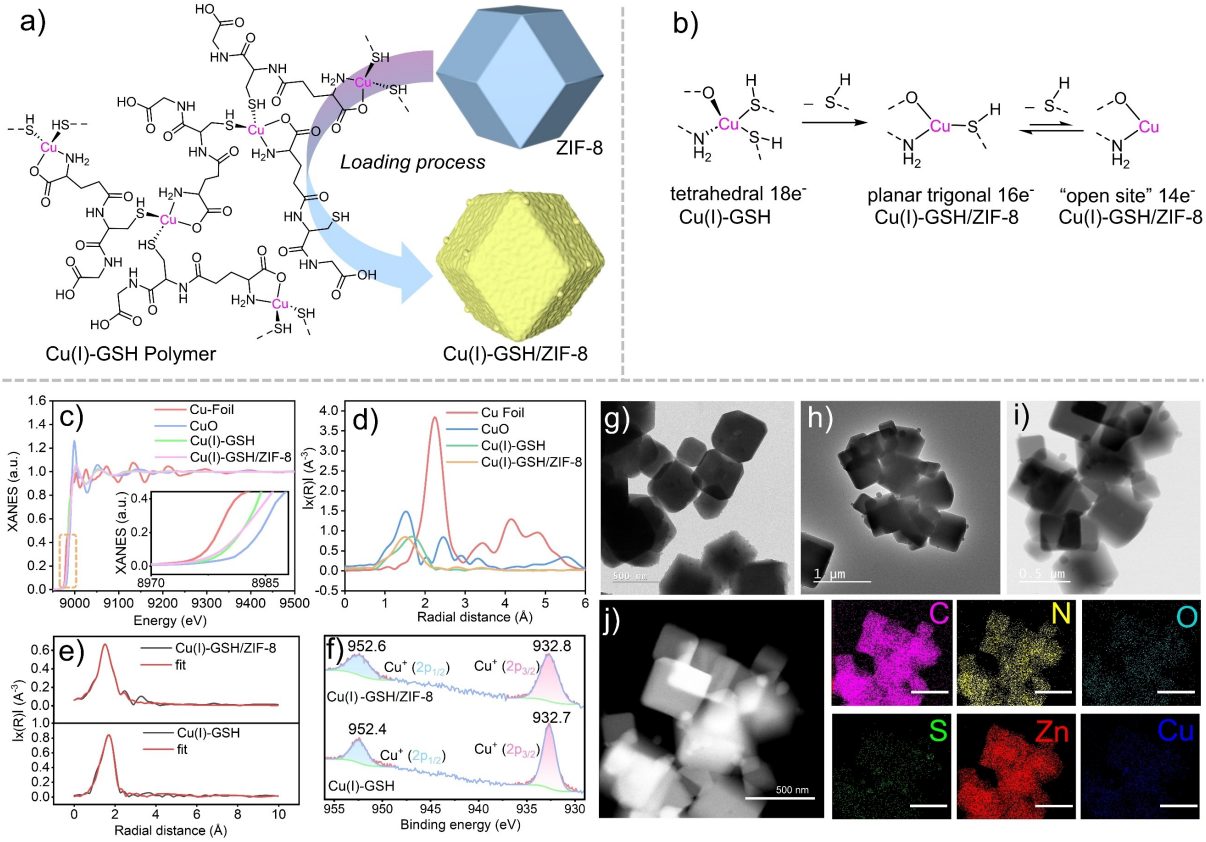

Figure 1. a) Proposed structures of the supramolecular metallopolymer Cu(I)-GSH and Cu(I)-GSH /ZIF/8. b) Coordination changes at the Cu(I) sites. Due to severe bulk around Cu, the weakly bonded thiol (2-electron ligand) readily dissociates in Cu-GSH/ZIF-8 in which additional steric constraints are imposed due to adsorption on ZIF-8 in the solid state. Substrate activation may occur by planar trigonal 16e Cu(I) species, possible after full thiol decoordination and ZIF-8 imidazole coordination. Here, the 18-electron ($18e^-$) abbreviated structure (left) represents the Cu sites in Figure 1a. c) Cu K-edge XANES. The inserted figure is the enlarged region of the orange frame of Figure 1c, showing that the oxidation state of the Cu catalysts is intermediate between 0 and 2. d) Fourier-transformed EXAFS spectra for the Cu K-edge of the sample. e) Corresponding EXAFS fitting curves of Cu(I)-GSH and Cu(I)-GSH /ZIF-8 at R space. f) Cu 2p XPS of Cu(I)-GSH (bottom) and Cu(I)-GSH/ZIF-8 (top). Corresponding TEM (g), HR-TEM (h, i), HAADF-STEM (j) and EDS mapping images of Cu(I)-GSH/ZIF-8 (scale bar: 500 nm).

with Cu. The Gly CO_2H (infrared: 1720 cm^{-1}, Figure S5) remains in polymeric Cu(I)-GSH that is only very weakly soluble in water and ethanol, contrary to zwitterionic GSH. The Cu(I) coordination[12] is tetrahedral due to the absence of ligand-field stabilization energy,[13] becoming planar trigonal in Cu(I)-GSH/ZIF-8, i.e. ideal for substrate coordination and activation.

Elemental C, H and N analysis shows a Cu(I): GSH stoichiometry close to 1:1, confirmed by inductively coupled plasma (ICP) Cu analysis (Table S2 and S3). Cyclic voltammetry in DMF shows the expected irreversible Cu(I) oxidation wave, unlike in Cu_4 clusters,[14] around 0.65 V vs. saturated calomel electrode (SCE, Figure S9). XPS confirms the presence of C, N, O, S and Cu elements in Cu(I)-GSH, and one more element, Zn, is shown in Cu(I)-GSH/ZIF-8 (Figure S10 and S11), in line with energy-dispersive spectroscopy (EDS) mapping images. XPS of Cu 2p (Figure 1f) shows Cu(I) oxidation state in Cu(I)-GSH (two peaks at 952.4 and 932.7 eV for Cu 2p1/2 and 2p3/2 respectively, absence of Cu(II) satellite peak around 942 eV, and a peak at 916 eV for Cu LMM Auger spectra; see Figure S10e).[15] After loading onto ZIF-8, the Cu(I) oxidation state remains unchanged, just with a 0.2 eV left shift to 952.6 eV and another 0.1 eV shift to 932.8 eV due to the interaction between Cu(I)-GSH and the ZIF-8 N atoms (Figure 1f). TEM, high-resolution TEM, high-angle annular dark-field scanning TEM (HAADF-STEM) and EDS mapping images confirm the loading of Cu(I)-GSH onto ZIF-8 (Figure 1g–i and S2).

The Brunauer-Emmet-Teller (BET) surface and pore volume of ZIF-8 hardly undergo any change from 1260.0 $m^2 \cdot g^{-1}$ and 0.633 $cm^3 \cdot g^{-1}$, before, to 1251 $m^2 \cdot g^{-1}$ and 0.626 $cm^3 \cdot g^{-1}$, respectively, after introduction of 0.3 wt % Cu(I)-GSH, and 1256.4 $m^2 \cdot g^{-1}$ and 0.637 $cm^3 \cdot g^{-1}$ after introduction of 0.45 wt % Cu(I)-GSH (Table S4 and Figure S12), showing Cu(I)-GSH polymer loading onto ZIF-8, not inside ZIF-8. Compared to the X-ray diffraction (XRD) pattern of ZIF-8 (Figure S13), Cu(I)-GSH/ZIF-8 with 0.3 wt % and 0.45 wt % of Cu exhibits similar shapes to that of ZIF-8, indicating that the morphology of ZIF-8 is unchanged after introduction of Cu(I)-GSH. Interestingly, the EXAFS data show that, upon adsorption onto ZIF-8, the Cu(I) coordination number decreases upon loss of one thiol ligand involving a low energy gap of <10 kcal/mol, from density functional theory (DFT) calculation, to planar tricoordinate Cu(I), favoring catalytic substrate coordination (Figure 1b). ZIF-8 not only acts as a support in Cu(I)-GSH/ZIF-8, but also as a CO_2 capping agent promoting its diffusion to substrates,[6] improving CO_2 fixation catalysis.

Both Cu(I)-GSH and Cu(I)-GSH/ZIF-8 in 0.39 resp. 0.47 mmol% catalyze the carboxylation of phenylacetylene, PhC≡CH, to PhC≡CCO_2H, both in 98 % yield of isolated product, in DMF with Cs_2CO_3 (1.5 equiv.) at 80 °C in 1d at atmospheric CO_2 pressure (balloon, Table S5). Optimization with Cu(I)-GSH/ZIF-8 provides a 94 % yield in 6 h, and under these conditions, it was reused 10 times without obvious decrease in catalytic activity (Figure S14a). Furthermore, after removing Cu(I)-GSH/ZIF-8 (Figure S14b), the reaction no longer works, which shows the absence of catalyst leaching. Various techniques were employed to analyze the recovered catalyst after 10 catalytic cycles to confirm their structural stability and phase purity. The XRD pattern of the recycled Cu(I)-GSH/ZIF-8 (Figure S13) matches well with that of the fresh sample. The reused catalyst shows a slight decrease in the BET surface area (1050.7 $m^2 \cdot g^{-1}$, Table S4, entry 2 vs. 3) implying preservation of the ZIF-8 structure morphology even after 10 catalytic cycles. The recycled Cu(I)-GSH/ZIF-8 with slightly wider peaks in the range from 21 to 36 degrees than those of fresh catalyst is ascribed to some fractional loss of crystallinity of the ZIF-8 support after 10-time usage, consistent with HAADF-STEM and EDS mapping images (Figure S15). The oxidation state Cu(I) remained unchanged after 10 cycles (Figure S16e). Remarkably, Cu(I)-GSH/ZIF-8 was stored in air for several days before re-use, then still reproducibly providing 93 to 96 % yields, showing that Cu(I)-GSH/ZIF-8 presents excellent recyclability and very efficiently catalyzes the linear CO_2 carboxylation of terminal alkynes (Table S5, entry 9 and 10).

This carboxylation reaction was successfully extended under these conditions, (Eq.1) always in high yields around 90 %, to a variety of arylalkynes, containing electron-withdrawing or electron-releasing groups as well as to other alkynes and polyalkynes (Eq. 1, R = aryl, pyridyl, 2-thiophenyl, aryl ether, see compounds **1a**–**1n**, Table S6).

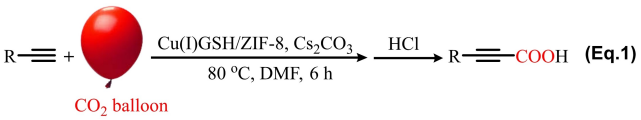

(Eq.1)

The catalyst Cu(I)-GSH/ZIF-8 was also employed in the cycloaddition of propargyl amines with CO_2. The conditions with N-propylamine were optimized with 5 % Cu(I)-GSH/ZIF-8 in 6 h at 60 °C, yielding 98 % of cyclic carbamate product (Table S7, R_1=CH_2Ph, R_2/R_3=H), as confirmed by ^{1}H NMR spectra (Figure S17). In comparison, Cu(I)-GSH, ZIF-8 and Cu/ZIF-8 taken separately only provided 23 %, 2 %, and 70 % respectively (Table S7), under similar conditions, hinting a significant synergy between Cu(I)-GSH and ZIF-8, and a different reactive site in Cu(I)-GSH/ZIF-8 from those involved in former CO_2 conversion reactions.[4–6]

With these optimized reaction conditions, various substrates were used to further verify the suitability of Cu(I)-GSH/ZIF-8 (Table 1). In the majority of cases (entry **2a**–**2h**), Cu(I)-GSH/ZIF-8 was smoothly applied in CO_2 conversion into 2-oxazolidinone synthesis with high yields under atmospheric pressure. Cu(I)-GSH/ZIF-8 shows a good tolerance to electron-withdrawing or electron-donating groups on the *N*-benzyl unit of propargylic amines (**2b** and **2c**). Although steric hindrance in *N*-(prop-2-yn-1-yl)cyclohexanamine (**2h**) induces a negative effect on conversion, a 90 % yield was obtained in 8 h. For *N*-(prop-2-yn-1-yl)aniline (**2i**), only a 55 % yield is obtained even after 3 days due to both the strong steric hindrance and the weak nucleophilicity of nitrogen directly connected to the phenyl group. For **2j**, to obtain a 94 % yield, 12 h are required owing to a significant decrease in the electrophilicity of internal alkyne carbon (≡C–CH), caused by the presence of

Table 1: Cycloaddition of various propargyl amine derivatives with CO_2.[a]

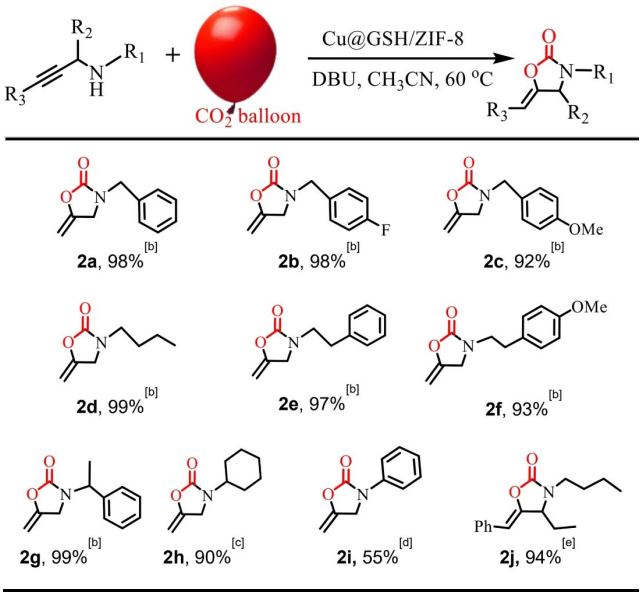

[a] Reaction conditions: substrates (0.2 mmol), 130 mg catalyst (5 mol% relative to substrate based on Cu), DBU (0.4 equiv.), CH_3CN (2 mL), CO_2 (balloon), 6 h. [b] Yield based on isolated product. [c] 8 h. [d] 3 d. [e] 12 h.

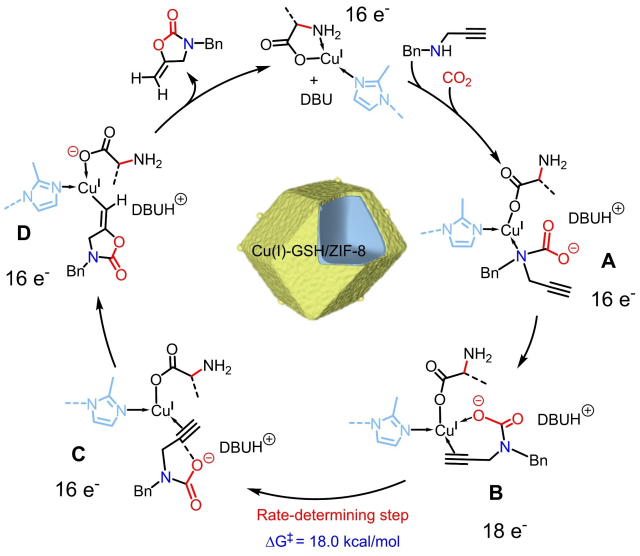

Figure 2. Reaction mechanism of carboxylative cyclization of N-benzyl-prop-2-yn-1-amine catalyzed by Cu(I)-GSH/ZIF-8; completed 16e⁻ Cu(I) state along the mechanism shows the role of the reversiible GSH chelation and ZIF-8 imidazole coordination. 3D model of Cu(I)-GSH/ZIF-8 in the center, ZIF-8 is in blue.

the phenyl group connected to the terminal alkyne. The catalyst Cu(I)-GSH/ZIF-8 was recycled up to 10 times with only minute reactivity loss (Figure S18a). Removal of Cu(I)-GSH/ZIF-8 from the medium stopped further reaction (Figure S18b), indicating absence of catalyst leaching. The XRD pattern of the recycled catalyst Cu(I)-GSH/ZIF-8 (Figure S13) is in line with that of the fresh sample, and the BET surface area of 1217.5 $m^2 \cdot g^{-1}$ for the recycled sample (Table S4, entry 4 vs. 5) was close to that of the parent sample (1256.4 $m^2 \cdot g^{-1}$). All the results above, XPS of Cu 2p (Figure S16f), HAADF-STEM and EDS mapping images (Figure S19) suggest that, even after 10 catalytic cycles, the original MOF structure and Cu(I) oxidation state were still retained. The above results indicate that Cu(I)-GSH/ZIF-8 effectively catalyzes the cycloaddition of propargylamines with carbon dioxide under 1 atm and mild conditions with excellent stability and reusability.

Based on these results and previous reports,[16] the proposed mechanism is shown in Figure 2 and S20. Following experiments, Cu 2-aminobutyrate (I) is first used as model catalyst in (DFT) calculations (Figure S20). Due to the steric hindrance of the GSH ligand, the substrate N atom favorably coordinates to Cu. Then, after deprotonation, N-carboxylation produces intermediate **A**. Subsequently, **A** easily isomerizes to C1-coordinated **B**. In the rate-limiting step, cyclization to **C** (Figure 2 and S20) occurs, and the formed intermediate **D** undergoes H transfer to regenerate **I** and the base, and releases the product. In order to clarify the effects of ZIF-8, catalyst coordination environment and electronic state, we constructed the new models 16e-$\mathbf{I^z}$ (imidazole coordinated Cu 2-aminobutyrate), 14e-$\mathbf{I^O}$ (cuprous acetate) and 16e-$\mathbf{I^{OZ}}$ (imidazole coordinated cuprous acetate) with the single O-coordination, O-NH_2 coordination and O(carboxyl)-N(imidazole) coordination, (Figure S21). Calculations indicated that the barriers of the cyclization step for $\mathbf{I^Z}$, $\mathbf{I^O}$, and $\mathbf{I^{OZ}}$ are similar to **I** (18.0 vs. 19.0 vs. 17.1 vs. 19.3 kcal/mol), in which imidazole coordination slightly reduced the energy barrier of the rate-limiting step. The synergy between Cu(I)-GSH and ZIF-8, characterized by slight shifts in the XPS data, partly resulted from local CO_2 concentration in ZIF-8 via its capture and sink capacity.[17] This synergy is shown by DFT calculation indicating lowering of the energy barrier of the rate-limiting cyclization step via imidazole coordination and by large carboxylation yield increase upon Cu(I)GSH adsorption onto ZIF-8.

In conclusion, the novel, remarkably robust, fully air stable heterogeneous Cu(I)-GSH/ZIF-8, in which the ZIF-8 framework stabilizes the bio-relevant supra-metallopolymer Cu(I)-GSH, is highly efficient for CO_2 conversion at atmospheric pressure into fine linear and cyclic chemicals. Compared with the catalyst Cu(I)-GSH alone that cannot be recycled, the heterogeneous "single-atom" catalyst Cu(I)-GSH/ZIF-8 shows excellent recyclability (at least 10 times) with synergetic effects detailed above between Cu(I)-GSH and the ZIF-8 support. This work involving the biosystem Cu(I)-GSH combines greenness and high efficiency. Contrary to the biological tetranuclear $Cu_4(I)(GSH)_6$ clusters and other known Cu_4 catalysts,[18] Cu(I)-GSH/ZIF-8 brings a new, counter-intuitive structure involving an extraordinarily robust, air-stable, yet coordinatively flexible supramolecular metallo-polymer with an active planar trigonal mononuclear Cu(I) catalytically active species, a bio-related concept that might be usefully extended to a number of other catalytic processes.

Supporting Information

Supporting Information (SI, 77 pages) contains details of the syntheses, characterization, and reactivity, including Figures S1–S22 and Tables S1–S7.

Acknowledgements

Financial support from Chinese Scientific Council (CSC, PhD grants to W. W. and T. W.), Universities of Bordeaux, Rennes, Anhui, and Toulouse, CNRS, CIC biomaGUNE, National Natural Science Foundation of China (U23A2090 and 22004001), Anhui Provincial Natural Science Foundation (2008085QB84), and Hefei advanced computing center is gratefully acknowledged.

Conflict of Interest

The authors declare no conflict of interest.

Data Availability Statement

The data that support the findings of this study are available from the corresponding author upon reasonable request.

Keywords: CO_2 · ZIF-8 · glutathione · alkyne · carboxylation · heterogeneous catalysis

[1] a) E. Falcone, F. Stellato, B. Vileno, M. Bouraguba, V. Lebrun, M. Ilbert, S. Morante, P. Faller, *Metallomics* **2023**, *15*, mfad040; b) E. Falcone, A. G. Ritacca, S. Hager, B. Vileno, Y. El Khoury, P. Hellwig, C. R. Kowol, P. Heffeter, E. Sicilia, P. Faller, *J. Am. Chem. Soc.* **2022**, *144*, 14758–14768; c) M. T. Morgan, L. A. H. Nguyen, H. L. Hancock, C. J. Fahrni, *J. Biol. Chem.* **2017**, *292*, 21558–21567.

[2] a) Q. Liu, L. P. Wu, R. Jackstell, M. Beller, *Nat. Commun.* **2015**, *6*, 2933; b) S. Wang, C. Xi, *Chem. Soc. Rev.* **2019**, *48*, 382–404; c) P. Kumar Sahoo, Y. Zhang, S. Das, *ACS Catal.* **2021**, *11*, 3414; d) Z. Zhang, Y. Zheng, L. Qian, D. Luo, H. Dou, G. Wen, A. Yu, Z. Chen, *Adv. Mater.* **2022**, *34*, 2201547.

[3] a) A. Tortajada, F. Juliá-Hernández, M. Börjesson, T. Moragas, R. Martin, *Angew. Chem. Int. Ed.* **2018**, *57*, 15948; b) C. S. Cao, S. M. Xia, Z. J. Song, H. Xu, Y. Shi, L. N. He, P. Cheng, B. Zhao, *Angew. Chem. Int. Ed.* **2020**, *59*, 8586; c) Y. Yu, L. M. Fang, Y. Liu, X. B. Lu, *ACS Catal.* **2021**, *11*, 8349–8357; d) X. R. Tian, X. L. Jiang, S. L. Hou, Z. H. Jiao, J. Han, B. Zhao, *Angew. Chem. Int. Ed.* **2022**, *61*, e202200123.

[4] a) J. K. Wu, R. T. He, S. L. Cheng, L. M. Han, N. Zhu, *ACS Sustainable Chem. Eng.* **2022**, *10*, 1214–1219; b) S. Kranjit, E. Tanaka, L. K. Shrestha, A. Nakayama, K. Ariga, K. Namba, *Catal. Sci. Technol.* **2022**, *12*, 3778–3785; c) Q. W. Song, R. Ma, P. Liu, K. Zhang, L. N. He, *Green Chem.* **2023**, *25*, 6538–6560; d) Z. Zhang, J. H. Ye, D. S. Wu, Y. Q. Zhou, D. G. Yu, *Chem. Asian J.* **2018**, *13*, 2292–2306; e) J. H. Ye, T. Ju, H. Huang, L. L. Liao, D. G. Yu, *Acc. Chem. Res.* **2021**, *54*, 2518–2531; f) Z. Y. Bo, S. S. Yan, T. Y. Gao, L. Song, C. K. Ran, Y. He, W. Zhang, G. M. Cao, D. G. Yu, *Chin. J. Catal.* **2022**, *43*, 2388–2394; g) M. Miao, L. Zhu, H. Zhao, L. Song, S. S. Yan, L. L. Liao, J. H. Ye, Y. Lan, D. G. Yu, *Sci. China Chem.* **2023**, *66*, 1457–1466.

[5] a) R. Freund, O. Zaremba, G. Arnauts, R. Ameloot, G. Skorupskii, M. Dincă, A. Bavykina, J. Gascon, A. Ejsmont, J. Goscianska, M. Kalmutzki, U. Lächelt, E. Ploetz, C. S. Diercks, S. Wuttke, *Angew. Chem. Int. Ed.* **2021**, *60*, 23975; b) S. Daliran, A. Oveisi, Y. Peng, A. López-Magano, M. Khajeh, R. Mas-Ballesté, J. Alemán, R. Luque, H. Garcia, *Chem. Soc. Rev.* **2022**, *51*, 7810; c) Q. Wang, D. Astruc, *Chem. Rev.* **2020**, *120*, 1438–1511.

[6] A. L. Gu, Y. X. Zhang, Z. L. Wu, H. Y. Cui, T. D. Hu, B. Zhao, *Angew. Chem. Int. Ed.* **2022**, *61*, e202114817.

[7] a) H. L. Karlsson, P. Cronholm, J. Guvtafsson, L. Moeller, *Chem. Res. Toxicol.* **2008**, *21*, 1726–1732; b) D. Tang, X. Chen, G. Kroemer, *Cell Res.* **2022**, *32*, 417–418.

[8] a) E. Assadian, M. H. Zarei, A. G. Gilani, M. Farshin, H. Degampanah, J. Pourahmad, *Biol. Trace Elem. Res.* **2018**, *184*, 35356; b) V. Kumar, S. Pandita, G. P. S. Sidhu, A. Sharma, K. Kannah, P. Kaur, A. S. Bali, R. Setia, *Chemosphere* **2021**, *262*, 127810.

[9] X. Jia, J. Li, E. Wang, *Small* **2013**, *9*, 3873–3879.

[10] a) K. S. Park, Z. Ni, A. P. Cote, J. Y. Choi, R. D. Huang, H. K. Chae, M. O'Keeffe, O. M. Yaghi, *Proc. Natl. Acad. Sci. USA* **2006**, *103*, 10186–10191; b) C. Wang, Q. Wang, F. Fu, D. Astruc, *Acc. Chem. Res.* **2020**, *53*, 2483–2493.

[11] J. Li, J. Wang, H. Li, N. Song, D. Wang, B. Z. Tang, *Chem. Soc. Rev.* **2020**, *49*, 1144–1171.

[12] a) B. Ravel, M. Newville, *J. Synchrotron Radiat.* **2005**, *12*, 537–541; b) D. C. Koningsberger, R. Prins, *X-ray Absorption: Principles, Applications, Techniques of EXAFS, SEXAFS, and XANES, Vol. 92*, Wiley **1988**, pp. 321–372; c) J. J. Rehr, R. C. Albers, *Rev. Mod. Phys.* **2000**, *72*, 621–654.

[13] L. Yang, D. R. Powel, R. P. Hauser, *Dalton Trans.* **2007**, 955–964.

[14] a) H. Tsurugi, Y. Ikeda, K. Shinohara, S. Shirase, N. Toya, S. Tanaka, K. Mashima, *Inorg. Chem.* **2019**, *58*, 12565–12572; b) R. N. Yang, Y. A. Sun, Y. M. Hou, X. Y. Hu, D. M. Jin, *Inorg. Chim. Acta* **2000**, *304*, 1–6.

[15] a) K. J. Koski, J. J. Cha, B. W. Reed, C. D. Wessells, D. Kong, Y. Cui, *J. Am. Chem. Soc.* **2012**, *134*, 7584–7587; b) Y. Sohn, D. Pradhan, L. Zhao, K. T. Leung, *Electrochem. Solid-State Lett.* **2012**, *15*, K35–K37.

[16] Y. Zhao, J. Qiu, L. Tian, Z. Li, M. Fan, J. Wang, *ACS Sustainable Chem. Eng.* **2016**, *4*, 5553–5560.

[17] a) X. Gong, Y. Wang, T. Kuang, *ACS Sustainable Chem. Eng.* **2017**, *5*, 11204; b) R. Yang, Y. Fu, H. Wang, D. Zhang, Z. Zhou, Y. Cheng, X. Meng, Y. He, Z. Su, *Chem. Eng. J.* **2022**, *450*, 138040.

[18] S. L. Hou, J. Dong, X. L. Jiang, Z.-H. Jiao, B. Zhao, *Angew. Chem. Int. Ed.* **2019**, *58*, 577–581.

Manuscript received: April 22, 2024
Accepted manuscript online: June 17, 2024
Version of record online: August 2, 2024